Hot Water Molecules from Dissociative Recombination of D_3O^+ with Cold Electrons

H. Buhr,[1,2,*] J. Stützel,[1] M. B. Mendes,[1] O. Novotný,[1,3] D. Schwalm,[1,2] M. H. Berg,[1] D. Bing,[1] M. Grieser,[1] O. Heber,[2] C. Krantz,[1] S. Menk,[1] S. Novotny,[1] D. A. Orlov,[1] A. Petrignani,[1] M. L. Rappaport,[2] R. Repnow,[1] D. Zajfman,[2] and A. Wolf[1]

[1]*Max-Planck-Institut für Kernphysik, 69117 Heidelberg, Germany*
[2]*Weizmann Institute of Science, P.O. Box 26, 76100 Rehovot, Israel*
[3]*Columbia Astrophysics Laboratory, MC5247, 550 West 120th Street, New York, New York 10027, USA*
(Received 27 April 2010; published 3 September 2010)

Individual product channels in the dissociative recombination of deuterated hydronium ions and cold electrons are studied in an ion storage ring by velocity imaging using spatial and mass-sensitive detection of the neutral reaction fragments. Initial and final molecular excitation are analyzed, finding the outgoing water molecules to carry internal excitation of more than 3 eV in 90% of the recombination events. Initial rotation is found to be substantial and in three-body breakup strongly asymmetric energy repartition among the deuterium products is enhanced for hot parent ions.

DOI: 10.1103/PhysRevLett.105.103202 PACS numbers: 34.80.Lx, 34.80.Gs, 34.80.Ht

In ionized media of low density and temperature an important source of water molecules is oxygen ion chemistry in repeated [1] reactions with molecular hydrogen, leading to the hydronium ion H_3O^+. This ion forms neutral water in one of the product channels of its dissociative recombination (DR) [2] with an electron, accompanied by an energy release of ~6 eV. Rate and branching ratios of this reaction as well as the excitation of the products are of basic importance for understanding the role of water molecules in astrophysical molecular clouds [3], comets [4], and planetary atmospheres [5]. Radiation by water molecules, following their production by DR of H_3O^+, promotes the cooling of dense molecular clouds [3], might explain unusual hot bands in recent cometary observations [6], and has been suggested as the origin of infrared laser action seen from water laboratory plasma [7]. Quantum chemical calculations [8–10] suggest that the incident electron is first captured in predissociating Rydberg states of the neutral H_3O radical [11]. For H_3O states bound by ~3 eV, probably below the Rydberg states governing the DR process, the predissociation into the $H_2O + H$ channel was studied recently [12] by H_3O^+ charge exchange on Cs, revealing vibrational excitation of the H_2O fragment of ~1–2 eV. The DR of H_3O^+ and its deuterated analogues was studied in flowing afterglow experiments [3,13] and at ion storage rings [14–17]. Most of these experiments [15,16] agree at a branching ratio for the water product channel of 17%–25%, except for one earlier result [3] of only 5%. The excitation of the OH product was investigated in flowing afterglows by laser-induced fluorescence [13], while a storage-ring experiment [17] recently analyzed the OH product excitation by fragment imaging.

Coincidence imaging of reaction fragments from fast overlapping molecular ion and electron beams in an ion storage ring has been established for exploring the molecular breakup in DR [2]. However, the imaging detectors used so far, based on electron multiplier plates, exhibit detection efficiencies for individual particles well below unity and give signals which cannot be correlated to their masses; hence, neither individual fragment masses nor the number of fragments following a DR event can be safely assigned if polyatomic ions are studied. We overcome this limitation by applying a multistrip surface-barrier detector [18] to determine individually, at high event rate and spatial resolution, the fragment translational energies, which in fast-beam imaging are proportional to their masses. Because of the intrinsic near-unity efficiency of the detector, the fragment multiplicity of an event and the fragment momenta in the plane transverse to the beam direction can be efficiently and reliably reconstructed for all DR product channels. Strongly improving the insight into this process from ion storage-ring experiments, this not only reveals the branching ratios between the individual DR product channels and the excitation carried by the atomic and molecular fragments, but also allows us to gain information on the initial excitation of the parent molecules.

We choose to study the deuterated species D_3O^+ and keep a fast beam of these ions in a storage ring for times up to 20 s to allow them to thermalize with the room-temperature environment. On a part of its orbit, the ion beam is merged with a velocity-matched cold electron beam. Applying the mass-sensitive detector, we image the resulting DR events leading into the highly exothermic two-body fragment channel $D_2O + D$ and find product kinetic energies much below the reaction energy release, implying a high internal excitation of the D_2O product of >3 eV. Through the energies of fragments in channel $OD + D + D$, the new detection technique also unambiguously reveals that the long-time storage of the D_3O^+ ions does not prevent them from keeping a high initial excitation. Analysis of the three-body breakup finally shows preferred geometries suggesting that a substantial part of

the OD + D + D events for hot parent ions occurs via a two-step process through excited, rapidly predissociating water molecules. The ensemble of results sheds light on the dissociative dynamics induced by cold electron collisions with hydronium ions, and at the same time illuminates the advantage of the recently introduced multistrip detector for studying the DR of polyatomic molecular ions.

The experiment is performed at the heavy ion storage ring TSR using a D_3O^+ beam of $E_B = 4.23$ MeV kinetic energy. The D_3O^+ ions are produced with a Penning ion source in a 2 MeV electrostatic accelerator and, after injection into the TSR, are brought to the final energy by synchrotron acceleration within ~3 s. The stored ion beam is merged over 1.1 m with a velocity-matched electron beam in the TSR electron target section (ETS) [19]. This beam from a cryogenic photocathode [20] has a kinetic temperature of ~10 K in the comoving reference frame and a typical density of $\sim 5 \times 10^6$ cm^{-3}. Phase-space cooling of the polyatomic ions by the electron beam occurs within 7 s and results in an ion beam diameter of <1 mm. Neutral DR fragments, separated from the circulating ion beam at the next storage-ring dipole, hit the recently introduced energy-sensitive multistrip detector EMU [18] mounted 941 cm from the center of the ETS. The pulse heights of the hits on the 10×10 cm^2 detector are read out using 128 vertical and 128 horizontal strip electrodes evaporated onto the front and back sides of the detector, respectively, and processed [18] to determine the masses m_i and transverse positions $\vec{r}_i$ of the individual fragments i. With the average velocities of the merged beams being equal, the collision energies amount to ~1 meV because of the finite temperature of the electron beam. At these collision energies the DR of D_3O^+ leads to three fragment channels as listed in Table I.

The background from charge-transfer collisions of D_3O^+ with the residual gas relative to the DR signal rate was <0.1%, found by offsetting the beam velocities for a collision energy of ~1 eV, where the D_3O^+ DR cross section is very small. All results are obtained for storage times of 15–20 s but differ only little for times >10 s.

For each event the c.m. position $\vec{r}_{cm} = \sum_i \vec{r}_i m_i / M$ in the detector plane and the total detected mass $M = \sum_i m_i$ are determined. For DR events, identified by requiring $M =$ 22 amu, the c.m. positions lie within a spot of only ~1 mm diameter, which reflects the small diameter and divergence of the phase-space cooled ion beam. For all fragment channels we then obtain the mass-weighted total squared distances D^2 from the projected squared fragment distances $\hat{d}_i^2 = (\vec{r}_i - \vec{r}_{cm})^2$ by $D^2 = \sum_i m_i \hat{d}_i^2 / M$ [18]. For a given distance S between the interaction point and the EMU detector, $D^2 = S^2 E_{k,\perp} / E_B$. Here $E_{k,\perp}$ is the transverse kinetic energy, which depends on the full kinetic energy release (KER) E_k as well as on the orientation of the fragment momenta in the c.m. frame; in particular, $E_{k,\perp} = E_k$ if all fragments are emitted in a plane perpendicular to the beam direction.

TABLE I. Channels c of the studied D_3O^+ DR with their energy releases E_c from the D_3O^+ ground state (revised from Ref. [15], ±0.1 eV [21]), and measured branching ratios.

Channel	Energy release (eV)	Branching fraction
$D_2O + D$	6.36	0.165(20)
$OD + D_2$	5.72	0.125(10)
$OD + D + D$	1.17	0.710(20)

At zero offset between the average beam velocities an isotropic distribution of breakup directions in the c.m. frame is expected, as also confirmed by previous DR measurements on diatomic ions [22]. Assuming, in addition, the fragment momentum geometries in the three-body channel to be equally distributed in phase space, and averaging over the interaction region, we can simulate for each channel the expected distributions $P(D^2; E_k)$ for a given KER E_k. The Monte Carlo based simulations also take into account the slightly different fragment detection efficiencies [18] caused by the detector geometry, the energy resolution, and the finite strip width of 760 μm, which occasionally may lead to a misassignment of OD + D + D as D_2O + D or OD + D_2. Branching ratios determined with the present technique are published in Ref. [23] together with those at higher collision energies up to 20 eV.

Examples of measured D^2 distributions are shown in Fig. 1. To analyze the KER reflected by them, each D^2 distribution was fitted by a sum $\sum_j \alpha_j \tilde{P}(D^2; (E_k)_j)$ of contributions for a set of energy bins $(E_k)_j$, varying the relative strengths α_j. The functions $\tilde{P}(D^2; (E_k)_j)$, normalized over D^2, were obtained by integrating $P(D^2; E_k)$ over the respective energy bin ranges. The bins in E_k and their relative strengths after overall normalization are displayed in Fig. 2, representing the derived KER histograms.

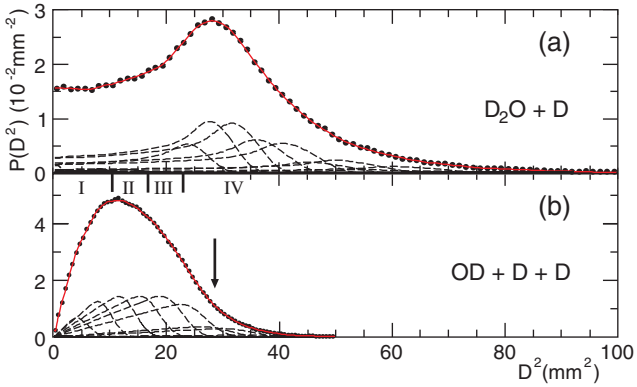

FIG. 1 (color online). Measured, normalized D^2 distributions (dots) for the DR product channels D_2O + D (a) and OD + D + D (b) with fits (solid lines) of the superimposed contributions (dashed lines) described in the text. In (b) the arrow marks the highest D^2 of OD + D + D expected for cold D_3O^+ ions; Roman numerals mark D^2 ranges applied below.

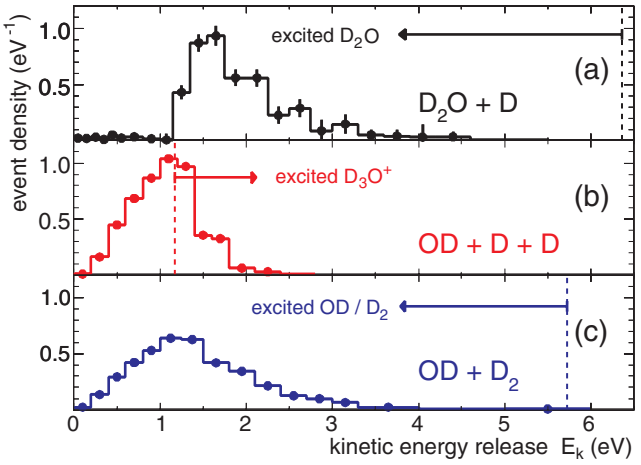

FIG. 2 (color online). Normalized kinetic energy release histograms derived from the D^2 distributions for the three DR fragment channels of D_3O^+; dashed lines mark the reaction energy releases E_c.

Most surprisingly, in the water producing DR channel [Fig. 2(a)] only a small part of the available energy is released as kinetic energy; in fact more than 90% of these events occur with KER deficits of >3 eV compared to the maximum available energy of 6.36 eV (D^2 up to 150 mm^2 in Fig. 1). Moreover, a remarkable sharp cutoff occurs at $E_k = E_{\mathrm{OD,D,D}} = 1.17$ eV, where the deficit coincides with the dissociation energy of D_2O. On the other hand, it follows from the KER spectrum deduced for the three-body channel OD + D + D [Fig. 2(b)] that more than 30% of all DR events have a KER exceeding the channel energy release $E_{\mathrm{OD,D,D}}$ by up to ~1 eV. Moreover, energy releases below 1.17 eV are observed, indicating the production of OD fragments with some internal excitation. The KER histogram for the second two-body channel OD + D_2, Fig. 2(c), also reveals a large KER deficit with respect to the channel energy release of $E_{\mathrm{OD,D_2}} = 5.72$ eV. In the KER histogram of this channel structures related to the opening of the OD + D + D (1.17 eV), O + D + D_2 (1.25 eV), and the OD* + D (1.67 eV) channels (the star denoting the first excited electronic state) can occur, if at least one of the resulting molecular fragments does not carry a high, broadly distributed rovibrational excitation. The maximum at $E_k \sim 1.2$ eV, close to both $E_{\mathrm{OD,D,D}}$ and $E_{\mathrm{O,D,D_2}}$, suggests that indeed one of the molecular fragments of this channel is only weakly excited and that the branching to OD* is minor. As previous measurements [13,17] indicate that OH fragments from the DR of H_3O^+ are mostly in lower vibrational states ($v \lesssim 3$), we attribute only a moderate excitation to OD while inferring that the D_2 fragments carry most of the KER deficit as internal energy.

The large KER deficit of >3 eV for most of the events in the D_2O + D channel points to a high, predominantly vibrational excitation of the D_2O molecules. The most striking argument for this is the excellent agreement of the minimum KER observed in Fig. 2(a) with the expected stability limit of D_2O. In principle, the missing KER might also be caused by radiative emission from high Rydberg states of the D_3O radical, likely to be formed in the initial phase of DR, to lower D_3O levels with less breakup energy towards D_2O. In fact, the lowest (3s) state of the D_3O radical is calculated [11] to lie ~1 eV above the D_2O + D threshold, not far from the observed minimum KER. However, the recent charge-exchange measurements [12] on H_3O^+ find very few signs, if any, of radiative decay for the lower H_3O levels studied.

The only viable explanation of the energy excess in the three-body channel is a significant excitation of the D_3O^+ ions even after >15 s of storage. Similar excess projected distances of three-body breakup products from the DR of H_3O^+ were in recent work [17] explained by background from residual gas collisions. Disregarding such events in the analysis, it was concluded that the H_3O^+ beam was internally thermalized to the 300 K blackbody field. However, in our case the measured low background level clearly rules out such an explanation. For all vibrational modes of D_3O^+, the calculated transition dipoles [24] imply radiative level lifetimes of <1 s. Hence, we conclude that the D_3O^+ ions are excited rotationally. Assuming the DR cross section to be independent of angular momentum we find a rotational temperature near 3500 K. High initial rotational excitation is known to occur through reactive collisions in the plasma-type ion sources used here as well as in most previous storage-ring DR measurements on polyatomic ions. While the long persistence of such an excitation is unanticipated considering the predicted subsecond radiative lifetimes [25] in the inversion-rotation spectrum even down to <0.05 eV, long-lived rotational levels are in fact conceivable considering the angular momentum selection rules governing the decay of rotating D_3O^+ [26].

For the OD + D + D channel also the three-body fragmentation geometries were analyzed. As previously established for the DR of triatomic ions [18,27], Dalitz coordinates defined by [18] $Q_1 = (m_D^2/m_{OD}M)^{1/2}(\hat{d}_{D_2}^2 - \hat{d}_{D_1}^2)/3D^2$ and $Q_2 = (m_{OD}/3m_D)(\hat{d}_{OD}^2/D^2) - 1/3$ are used to represent the measured projections of the fragment velocities in the detector plane. Histograms in Q_1, Q_2 are built for different D^2 ranges while taking into account the symmetry of the system as well as the properties of the EMU detection system [18]. They are normalized by corresponding histograms calculated for breakup geometries equally distributed in phase space. The resulting Dalitz ratio plots show a remarkable dependence on the D^2 cuts, changing from nearly flat [see Fig. 3(a)] to clearly structured [see Fig. 3(b)]. At the highest D^2, where the D_3O^+ ions undergoing DR are presumably strongly rotating, we find a local enhancement of up to 40% in the region of the Dalitz ratio plot where one D is released at much

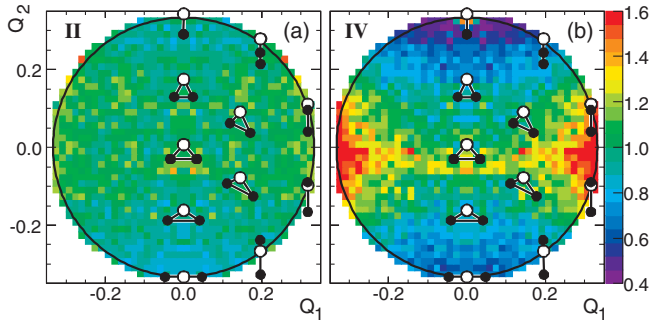

FIG. 3 (color online). Dalitz ratio plots for the three-body channel OD + D + D for two different D^2 ranges marked by Roman numerals and defined in Fig. 1(b).

smaller velocity than the other ($|Q_1| \approx 1/3$). One possible explanation for such a geometric preference is a two-step fragmentation via an intermediate, strongly vibrating D_2O fragment: at the high D^2 where the enhancement occurs, a strongly vibrating D_2O product can be expected to carry also considerable rotational energy left over from that of the parent ion. This could populate levels behind a rotational barrier, whose rotational predissociation [28] would produce slow D fragments in a second decay step.

The results demonstrate the large benefits to be gained from individual fragment mass assignment in molecular breakup imaging. Since investigations of DR and its final channels often aim at cold astrophysical media, the possibility of verifying the internal excitation of polyatomic parent ions will be valuable for future storage-ring DR measurements on them. The denser environment of flowing afterglow experiments [3,13] would avoid rotational excitation of the parent ions by collisional relaxation. In fact, somewhat lower branching ratios towards water were seen in these experiments which, however, in the light of the present measurements could be caused by collisional dissociation of the highly excited water products in this denser environment. Taken that the vibrational D_2O product excitation seen in our measurements by far exceeds the initial rotational energy, we rather consider that the branching ratios and product excitation reflect the predissociation dynamics of the D_3O radical formed in the initial recombination step, and we do not expect the basic character of the fragmentation dynamics towards $D_2O + D$ to be changed fundamentally through the presence of rotation in the D_3O^+ parent ion. Hence, our observations give strong direct evidence that water molecules produced by the DR of hydronium ions with cold electrons have a highly inverted vibrational population, experimentally reproducing the mechanism that makes DR of H_3O^+ a likely source of hot-band emission from water in terrestrial and extraterrestrial cold-plasma environments. While theory [8,9] has already considered the production of excited H_2O through this process, the precise mechanisms leading to the extremely high excitation found here are left for future investigations.

Helpful discussions with A. E. Orel, P. Jensen, and S. Yurchenko are acknowledged. H. B. acknowledges partial support by the German Israeli Foundation for Scientific Research and Development (G.I.F.) under Grant No. I-900-231.7/2005 and by the European Project ITS LEIF (HRPI-CT-2005-026015). O. N. was supported in part by the U.S. NSF Astronomy and Astrophysics. D. S. acknowledges support from the Weizmann Institute through the Joseph Meyerhoff program. Support by the Max-Planck-Society is acknowledged.

*Corresponding author.
henrik.buhr@mpi-hd.mpg.de

[1] E. Herbst and W. Klemperer, Astrophys. J. **185**, 505 (1973).
[2] M. Larsson and A. E. Orel, *Dissociative Recombination of Molecular Ions* (University Press, Cambridge, 2008).
[3] T. L. Williams *et al.*, Mon. Not. R. Astron. Soc. **282**, 413 (1996).
[4] N. Dello Russo *et al.*, Astrophys. J. **621**, 537 (2005).
[5] O. Witasse *et al.*, Space Sci. Rev. **139**, 235 (2008).
[6] R. J. Barber *et al.*, Mon. Not. R. Astron. Soc. **398**, 1593 (2009).
[7] E. A. Michael *et al.*, Chem. Phys. Lett. **338**, 277 (2001).
[8] A. E. Ketvirtis and J. Simons, J. Phys. Chem. A **103**, 6552 (1999).
[9] H. Tachikawa, Phys. Chem. Chem. Phys. **2**, 4327 (2000).
[10] M. Kayanuma, T. Taketsugu, and K. Ishii, Chem. Phys. Lett. **418**, 511 (2006).
[11] M. Luo and M. Jungen, Chem. Phys. **241**, 297 (1999).
[12] J. E. Mann *et al.*, J. Chem. Phys. **130**, 041102 (2009).
[13] T. Gougousi, R. Johnsen, and M. F. Golde, J. Chem. Phys. **107**, 2430 (1997).
[14] L. H. Andersen *et al.*, Phys. Rev. Lett. **77**, 4891 (1996).
[15] M. J. Jensen *et al.*, Astrophys. J. **543**, 764 (2000).
[16] A. Neau *et al.*, J. Chem. Phys. **113**, 1762 (2000).
[17] V. Zhaunerchyk *et al.*, J. Chem. Phys. **130**, 214302 (2009).
[18] H. Buhr *et al.*, Phys. Rev. A **81**, 062702 (2010).
[19] F. Sprenger *et al.*, Nucl. Instrum. Methods Phys. Res., Sect. A **532**, 298 (2004).
[20] D. A. Orlov *et al.*, J. Appl. Phys. **106**, 054907 (2009).
[21] R. J. Cotter and W. S. Koski, J. Chem. Phys. **59**, 784 (1973).
[22] Z. Amitay *et al.*, Phys. Rev. A **54**, 4032 (1996).
[23] O. Novotný *et al.*, J. Phys. Chem. A **114**, 4870 (2010).
[24] M. E. Colvin, G. P. Raine, H. F. Schaefer, III, and M. Dupuis, J. Chem. Phys. **79**, 1551 (1983).
[25] P. Botschwina, P. Rosmus, and E. A. Reinsch, Chem. Phys. Lett. **102**, 299 (1983).
[26] P. R. Bunker and P. Jensen, *Molecular Symmetry and Spectroscopy* (NRC Research Press, Ottawa, 1998).
[27] D. Strasser *et al.*, Phys. Rev. A **66**, 032719 (2002).
[28] A. Carrington, J. Buttenshaw, R. A. Kennedy, and T. P. Softley, Mol. Phys. **44**, 1233 (1981).